

**The dipeptidyl peptidase IV inhibitory activity and multifunctional antidiabetic properties of SQSPA: Structure – activity analysis evaluated with alanine scanning**

**Mohammed Auwal Ibrahim<sup>a,c\*</sup>, June C. Serem<sup>b</sup>, Megan J. Bester<sup>b</sup>, and Anabella R.M. Gaspar<sup>a</sup>**

*<sup>a</sup>Department of Biochemistry, Genetics and Microbiology, University of Pretoria, Pretoria 0002, South Africa*

*<sup>b</sup>Department of Anatomy, University of Pretoria, Pretoria 0002, South Africa*

*<sup>c</sup>Department of Biochemistry, Ahmadu Bello University, Zaria, Nigeria*

**\*Correspondence to:** Dr. Mohammed Auwal Ibrahim, Department of Biochemistry, Genetics and Microbiology, Faculty of Natural and Agricultural Sciences, University of Pretoria, Pretoria 0002, South Africa E mail: [mauwalibrahim@gmail.com](mailto:mauwalibrahim@gmail.com) or [maibrahim@abu.edu.ng](mailto:maibrahim@abu.edu.ng)

## Abstract

Type 2 diabetes is a multifactorial disease and drugs with multifunctional properties are required. The peptide, SQSPA, was reported to be a potent and gastrointestinally stable  $\alpha$ -glucosidase inhibitory peptide. In this study, the structure-activity relationship of this peptide was studied using alanine scanning. Four analogs; AQSPA, SASPA, SQAPA and SQSAA were designed and investigated for multifunctional antidiabetic effects. Molecular docking studies on human dipeptidyl peptidase-IV (DPP-IV) suggested that the binding affinities were in the order; AQSPA>SASPA>SQSPA>SQSAA>SQAPA while for *in vitro* DPP-IV inhibitory activity, it was SQSPA>SQSAA>AQSPA>SASPA>SQAPA. Enzyme kinetic studies revealed that the peptides are uncompetitive inhibitors with the exception of SQSAA and SQSPA. In 3T3-L1 differentiated adipocytes, SASPA was the only analog that significantly ( $p<0.05$ ) reduced and prevented lipid accumulation and did not induce cytotoxicity to differentiated 3T3-L1 cells. All peptides, especially SASPA scavenged methylglyoxal and peroxy radicals thereby preventing advanced glycosylated end products formation and oxidative stress. The nitric oxide scavenging activity of all peptides was comparable to IPI and glutathione. Findings indicate that the amide side chain of Q2 is probably the most critical functional group for modulating the multifunctional antidiabetic effects of SQSPA while SASPA has been identified, as a novel peptide with enhanced multifunctional antidiabetic activity.

**Key words:** Alanine scanning; SQSPA; Type 2 diabetes

## 1. Introduction

Peptides are a fascinating class of pharmaceutical agents that are biochemically and therapeutically distinct from small molecules [1]. Currently, peptide therapeutics are an important emerging market in the pharmaceutical industry with more than 60 peptide-based drugs approved by the FDA while 600 or more are at various phases of clinical and preclinical trials [2]. Indeed, peptide-based therapeutics have attracted a market of approximately 20 billion USD from drugs such as Fuseon (HIV), Captopril (hypertension), Zoladex (prostate cancer), Sandostatin – octreotide (acromegaly, endocrine tumors) and Copraxone (sclerosis) [3]. Furthermore, the high success rate of peptide-based drugs at the

clinical trial stage is attributed to high specificity, predictable metabolism in addition to a low incidence of side effects and/or toxicity [2]. The high toxicity of small molecules is often the main reason for their failure at the clinical trial stage. Conversely, the major limiting factors affecting the use of peptide therapeutics are poor oral bioavailability [4] and susceptibility to gastrointestinal enzymatic degradation [2]. However, note-worthy scientific advancements have been made to circumvent most of these therapeutic limitations [2, 4]. One of these scientific strategies is the design of peptides with sequences that are predicted to escape gastrointestinal digestion [5]. Subsequent structure-activity relationship studies of the peptide are essential to identify critical amino acid(s) needed for the therapeutic action(s). Both processes enable a rational approach to the development of peptide-based therapeutics. Luckily, the structure-activity relationship can be deduced via peptide scanning where systematic modification of each amino acid residue in a given peptide provides information on the role of a specific amino acid to the overall biological activity [3]. Among the different peptide scanning strategies, alanine scanning is the most commonly used because the substitution of a residue side chain by a methyl group provides an effective means to identify the side chains responsible for binding and pharmacological activity [6]. Moreover, this strategy has contributed to the development of therapeutically improved peptide analogs.

The Peptide Innovation for Early Diabetes Treatment (PIONEER) programme is the first clinical trial to investigate the therapeutic viability of a peptide-based antidiabetic candidate, semaglutinide [4]. However, at the different phases of the PIONEER trial, the drug presented severe adverse effects such as nausea and gastrointestinal discomfort [4, 7]. This clearly underscores the need for more drug discovery research to obtain a range of new peptide-based antidiabetic candidates. This is because diabetes mellitus affects 451 million people and the current global expenditure for people with the disease is estimated to be 850 billion USD [8]. The control of blood glucose level is the central focus of diabetes treatment and the inhibition of carbohydrate digestion enzymes such as  $\alpha$ -glucosidase and  $\alpha$ -amylase is one of the therapeutic options to achieve a favourable glycaemic control [9]. In a previous study, we identified from the literature, 43 fully sequenced peptides with  $\alpha$ -glucosidase inhibitory activity. *In silico* simulated gastrointestinal digestion with a combination of chymotrypsin, trypsin and pepsin in the BIOPEP database (<http://www.uwm.edu.pl/biochemia/index.php/en/biopep>) indicated that all the highly active peptides, except SQSPA, were gastrointestinally unstable [10]. Subsequently, alanine scanning strategy was used for structure-function analysis of SQSPA where an analog,

AQSPA, was identified to have a superior  $\alpha$ -glucosidase inhibitory activity than the parent peptide [11]. Also, the SQSPA analogs were predicted to be gastrointestinally stable to a combination of chymotrypsin, trypsin and pepsin in the BIOPEP database [11].

Type 2 diabetes (T2D) is a multifactorial disease that requires multiple therapeutic strategies for effective management. Apart from  $\alpha$ -glucosidase inhibitors, another important class of antidiabetic drugs is the dipeptidylpeptidase IV (DPP-IV) inhibitors which increase the half-life of incretin hormones and promote glucose-dependent insulin secretion [12], thereby regulating glucose homeostasis. T2D is also associated with dyslipidemia and obesity as a result of poor lipid metabolism and dysfunctional adipocyte differentiation [13], which increases the risk and complications associated with cardiovascular disease. Azul et al. [14] reported that T2D is associated with perivascular adipocyte dysfunction which contributes to oxidative stress, inflammation and dysfunction of the endothelium. Furthermore, diabetic vascular complications are associated with the accumulation of methylglyoxal (MGO) due to the exposure of endothelial cells to excessive hyperglycemia [15]. Consequently, this promotes the generation of advanced glycated end products (AGEs) and reactive oxygen species (ROS) which have been identified to be associated with the pathogenesis of T2D. Moreover, increased levels of nitric oxide (NO) are associated with endothelial dysfunction and cardiovascular complications, as demonstrated by a detailed systematic review and meta-analysis [16]. Based on the above, a peptide with the ability to target several aspects of the disease such as the DPP-IV, dyslipidemia and adipocyte differentiation, MGO accumulation and oxidative stress would be of pharmacological value and will improve patient outcome.

In our quest to gain further insights into the structure-activity relationship and improve the therapeutic potential of SQSPA, an alanine scanning strategy was used to design four peptide analogs of SQSPA. Then, the peptide and the analogs were evaluated for *in silico* and *in vitro* DPP-IV inhibitory activity, effects on adipocyte differentiation and lipid accumulation in addition to their ability to scavenge MGO, ROS and NO radicals.

## 2. Materials and methods

### 2.1 Chemicals and reagents

The peptide SQSPA along with its analogs AQSPA, SASPA, SQAPA and SQSAA were procured from Genscript (New Jersey, USA). Sigma-Aldrich Chemical Company (Johannesburg, South Africa) supplied kidney DPP-IV, diprotin A, Gly-Pro-p-nitroanilide, Dulbecco's modified Eagle's medium (DMEM), antibiotic solution (10000 units penicillin, 10 mg streptomycin, 25 µg amphotericin B per mL), isobutylmethylxanthine (IBMX), Oil Red O, rosiglitazone, dexamethasone, insulin, fluorescein, reduced glutathione (GSH), bovine serum albumin (BSA), 2,2'-azobis(2-amidinopropane) dihydrochloride (AAPH) and MGO. The 3-[4,5-dimethylthiazol-2-yl]-2,5-diphenyltetrazolium bromide (MTT), sodium nitroprusside, sulphanimide, N-(1-naphthyl)-ethylenediamine-dihydrochloride (NED) and dimethylsulfoxide (DMSO) were obtained from Merck (Johannesburg, South Africa) and foetal calf serum (FCS) was procured from Capricorn Scientific (GmbH, Germany), supplied by BIOCOM, South Africa.

### 2.2 Molecular docking with Autodock Vina

Initially, the five peptides were subjected to molecular docking analysis to enable the predictions of their binding potential towards human DPP-IV. To achieve this, the 3D crystal structure of the human DPP-IV complexed with diprotin A (PDB ID 1WCY resolved to 2.20Å by x-ray diffraction) was retrieved in PDB format from the protein data bank ([www.rcsb.org](http://www.rcsb.org)). Diprotin A along with other co-crystallized ligands were removed from the protein structure using UCSF chimera version 1.11.2 ([www.cgl.ucsf.edu/chimera/](http://www.cgl.ucsf.edu/chimera/)) [17]. Subsequently, the protein and the five peptide ligands were prepared for the molecular docking using the dock prep tool of the chimera software with all default parameters. Thereafter, the Autodock Vina tool [18] of the same software was used for the molecular docking of the PDB prepared versions of the protein and the peptide ligands. The grid sizes (xyz points) were set as 43.74, 47.51 and 66.02 while the grid centers were designated at dimensions (x, y and z) 45.30, 60.83 and 41.59. Other parameters of Autodock Vina in chimera were left as default. At the end of the docking, the minimum binding free energy for each of the peptides was recorded while the docking pose was extracted and aligned with the protein structure for the analysis of hydrogen bond interactions.

### 2.3 Peptide synthesis and preparation

Flexpeptide<sup>TM</sup> technology was used for the synthesis of SQSPA and the four analogs by GenScript while reverse phase high performance liquid chromatography and mass spectrometry were used by the manufacturer for the determination of the purity, molecular mass and amino acid analysis of the peptides. Stock peptide solutions were prepared in sterile deionized double distilled water.

### 2.4 DPP-IV inhibitory activity of the peptides and the mechanism of inhibition

The DPP-IV inhibitory activity was measured as earlier described [19]. Briefly, the peptides at final concentrations of 62.5-500  $\mu$ M were incubated with 0.02 U/mL DPP-IV (in 100 mM Tris-HCl buffer (pH 8.0)) at 37 °C for 60 min followed by the addition of 25  $\mu$ L of a 6 mM Gly-Pro-*p*-nitroanilide solution. The reaction mixture was then incubated at 37 °C for 60 min and the absorbance was measured at 405 nm (Spectramax paradigm multi-mode microplate reader, Molecular Devices LLC, USA). Diprotin A (IPI) was used as a positive control for the enzyme inhibition. The DPP-IV inhibitory activity was expressed as percentage of a control sample without the inhibitors which was calculated using the following formula:

$$\text{DPP – IV inhibitory activity (\%)} = \left(1 - \frac{A_s}{A_c}\right) \times 100$$

where  $A_s$  and  $A_c$  are the absorbance of sample and absorbance of control respectively. The concentrations of the peptides resulting in 50% inhibition of enzyme activity ( $IC_{50}$  values) were determined using the straight-line equations of the percentage inhibitory activity against the respective logarithm of peptide concentrations.

In order to determine the mode of inhibition towards the DPP-IV, the peptides were analyzed using enzyme inhibition kinetic experiments. These involve the same experimental protocol described above except that two fixed final concentrations of the peptides (250 and 500  $\mu$ M) with variable concentrations of Gly-Pro-*p*-nitroanilide (0.75 – 6 mM) were used. The data obtained were used to construct Lineweaver-Burk plots to determine the type of inhibition of the peptides against the DPP-IV.

### *2.5 Cell cultures and differentiation of 3T3-L1 cells*

The 3T3-L1 cells were procured from CELLONEX Separations at passage 39 and used for these experiments at passage 42-47. The cells were cultured in DMEM supplemented with 10% (v/v) FCS and 1% antibiotics (DMEM/FCS) at 37 °C in an atmosphere of 5% CO<sub>2</sub> grown to confluence, with splitting at 3-4 days intervals. Subsequently, the cells were induced to differentiate by seeding the pre-adipocyte cells at a concentration of  $1 \times 10^3$  per 100  $\mu$ L in a 96 well plate and were cultured until confluence was achieved after three days. On day 4, the cells were cultured in DMEM/FCS supplemented with final concentrations of 10  $\mu$ g/mL insulin, 25 mM IBMX, 50  $\mu$ M dexamethasone and 100  $\mu$ M rosiglitazone. This medium was replenished at 3 days intervals for 6 days. On day 10, the cells were cultured in DMEM/FCS supplemented with 10  $\mu$ g/mL insulin (no IBMX, dexamethasone and rosiglitazone added) for another 3 days. On day 14, the medium was changed to DMEM/FCS only. The presence of round cells rich in easily distinguishable fat globules observed with phase contrast microscopy confirmed differentiation. Undifferentiated/pre-adipocyte 3T3-L1 cells, were seeded at a concentration of  $4 \times 10^3$  per 90  $\mu$ L and left to attach overnight at 37°C, 5% CO<sub>2</sub>.

### *2.6 Prevention of lipid accumulation in 3T3-L1 differentiated adipocytes and Oil Red O staining assay*

Two experimental strategies were used to assess the anti-lipid formation effects of SQSPA and analogs in the differentiated 3T3-L1 adipocytes. The first strategy was to add 50 and 100  $\mu$ M peptide with the differentiation media at days 4, 7 and 10. The second strategy was to expose fully differentiated 3T3-L1 adipocytes to the peptides at a final concentration of 50 and 100  $\mu$ M peptide, for 24 h.

For both experiments, the adipocytes were stained with Oil Red O (ORO) and the effects of the peptides on lipid accumulation were determined. On completion of each experiment, the adipocytes were fixed with 2% (v/v) formaldehyde for 30 min at 37°C, and 5% CO<sub>2</sub>. The fixative was then discarded, the plate was dried and staining was achieved with freshly diluted ORO solution (0.5% ORO (w/v) in 60% isopropyl alcohol then further diluted 3:2 with ddH<sub>2</sub>O) for 30 min. The staining solution was removed and the cultures were rinsed with water and dried. Thereafter, images of the stained lipid droplets were captured using an Olympus microscope (Olympus, Tokyo, Japan). For quantification, the ORO dye was then extracted with 60% isopropanol and the absorbance was measured at 405 nm (BioTek plate

reader). The percentage lipid accumulation was calculated relative to the unexposed differentiated 3T3-L1 cells (100% lipid formation).

### *2.7 Cytotoxicity of peptides on the pre-adipocytes and adipocytes*

The cytotoxicity of the peptides towards both differentiated and undifferentiated 3T3-L1 cells was determined by exposing the pre-adipocytes and the adipocytes to 10  $\mu$ L of the peptide solution at 50 and 100  $\mu$ M final concentrations, for 24 h at 37°C, 5% CO<sub>2</sub>. Thereafter, cytotoxicity was evaluated with the MTT assay. Briefly, this involves addition of 10  $\mu$ L of a 1 mg/mL MTT solution to each well. After incubation for 3 h at 37 °C and 5% CO<sub>2</sub>, the medium was removed, and the plate was dried at room temperature. The formed purple formazan crystals were dissolved with 50  $\mu$ L 25% (v/v) DMSO in ethanol with shaking for approximately 3 min. The absorbance was measured at 570 nm (BioTek plate reader). Cell viability in the presence of peptides was expressed as a percentage relative to the control of either undifferentiated or differentiated cells (100% cell viability).

### *2.8 Scavenging effects of the peptides on methylglyoxal*

The MGO scavenging effect was assayed according to a modified method of Siddiqui et al. [20]. In this assay, 25  $\mu$ L of 56 mM MGO was mixed with 25  $\mu$ L of each peptide (31.25 – 250  $\mu$ M) (P + MGO) in a 96-well fluorescence plate followed by the addition of 50  $\mu$ L of 0.1 M phosphate buffer (pH 7.4) to achieve a final volume of 100  $\mu$ L per well. The plate was incubated at 37°C for 7 days in a sterile 5% CO<sub>2</sub> environment. The positive control contained 40 mg/mL of BSA, MGO and phosphate buffer pH 7.4 (BSA + MGO) while the vehicle control consisted of peptide and phosphate buffer (P). After incubation, the fluorescence was measured at an excitation wavelength (Ex) of 330nm and an emission wavelength (Em) of 420 nm using a FLUOstar OPTIMA plate reader (BMG labtechnologies, Offenburg, Germany) The amount of AGEs formed was expressed as a percentage change in fluorescence (P + MGO) - P relative to the positive control (BSA+ MGO) (100% AGE formation).

### *2.9 Oxygen radical absorbance capacity (ORAC) antioxidant assay*

The antioxidant capacity of the peptides was assayed using the ORAC method as described by Ou et al. [21]. Briefly, 165  $\mu$ L fluorescein (0.139 nM) was reacted with 10  $\mu$ L of each peptide (5-50  $\mu$ M, final concentration) in each well of a 96 well plate, followed by 25  $\mu$ L of a



0.24 mM AAPH solution. The fluorescence was immediately measured at an Ex and Em of 485 nm and 520 nm, respectively, every 60 sec for 120 min, to generate 120 cycles using a FLUOstar OPTIMA plate reader (BMG labtechnologies, Offenburg, Germany). The vehicle control contained fluorescein with ddH<sub>2</sub>O while the positive control contained only fluorescein with AAPH. Trolox was used at final concentrations of 0 – 50 μM to prepare a standard curve. The area under curve was calculated and the antioxidant activity of each peptide sample was expressed as μMTE.

### *2.10 Nitric oxide scavenging activity assay*

The ability of each peptide to directly scavenge NO was determined. In this assay, 10 μL of each of the peptide at a final concentration of 12.5-100 μM were added to 40 μL of a 5 mM sodium nitroprusside solution (dissolved in 0.1 M phosphate buffered saline and left to stand for 1 h in the light). After an incubation period at 37 °C for 1 h, NO levels were determined with the Griess assay [22]. This was achieved by adding 50 μL of Griess reagent (1% sulfanilamide and 0.1% NED in 2.5% (v/v) phosphoric acid) and the absorbance measured at 570 nm (BioTek plate reader). Glutathione (GSH) was used as a positive control. The amount NO scavenged by the peptides was expressed as a percentage relative to the control containing all reagents except peptide.

### *2.11 Statistical analysis*

For each experiment, two independent experiments were conducted. Also, triplicate determinations (n=3) were performed in each of the independent experiments. Hence, the results are presented as mean ± SD of the two independent experiments conducted in triplicate. The data were analyzed by using a statistical software package (SPSS for Windows, version 18, IBM Corporation, NY, USA) using Tukey's-HSD multiple range post-hoc test. Values were considered significantly different at  $p < 0.05$ .

### 3. Results

In order to establish the ability of SQSPA and its analogs to bind DPP-IV, the peptides were subjected to molecular docking analysis where substitution of S1 with alanine (AQSPA) was found to profoundly increase the binding affinity of the peptide (Table 1). Apart from the substitution of S3 for alanine (SQAPA), the alanine substitution tends to increase the binding affinity of SQSPA while substitution at position 4 had no effect. This might indicate that alanine substitution at S1 and Q2 positively affected the binding affinity towards the DPP-IV. Regarding the number of hydrogen bond interactions, alanine substitution at S1 still demonstrated the highest number of the interactions with 11 hydrogen bonds (Fig. 1) while substitution at positions 2 and 3 also increased hydrogen bond interactions. It was noteworthy that substitution of proline at position 4 (SQSAA) reduced the hydrogen bond interactions of the parent peptide (Fig. 1) indicating the need for the proline residue for such interactions. In the parent peptide, S1 was the only amino acid residue involved in all the three hydrogen bonds, but the substitution at position 1 altered that pattern where Q2 and A5 each mediated five of the interactions. Overall, Q2 and A5 were the most hydrogen bonded amino acid residues in the various alanine substitutions suggesting that these sites could be critical positions for hydrogen bond formation (Table 1). With the exception of substitution at position 3 (SQAPA), SQSPA and other analogs bind at the active site of the DPP-IV, though with varied conformations, suggesting that S3 might still be crucial for the binding of the peptide to the active site (Fig. 1). The interacting residues of DPP-IV with SQSPA were R125, N710 and Y547 but all the alanine substitutions on the peptide abolished the hydrogen bond interaction with N710 while the involvement of R125 was only maintained when S1 was substituted (AQSPA).

**Table 1.** Binding free energy (kcal/mol) and other docking results of SQSPA analogs with the human DPP-IV

Peptide ligand	Binding energy (kcal/mol)	Number of hydrogen bonds	Interacting residue of the peptide	Interacting residue of the DPP-IV	Hydrogen bond distance (Å)
SQSPA	-7.0	3	S1	R125	1.850
			S1	N710	2.233
			S1	Y547	1.873
AQSPA	-8.1	11	A5	R125	2.234
			A5	R125	2.688
			A5	R125	2.178
			A5	R125	2.475
			A5	H740	2.356
			S3	Y547	2.363
			Q2	F357	3.328
			Q2	E206	2.529
			Q2	R669	2.382
			Q2	R669	1.986
			Q2	E206	3.116
SASPA	-7.1	7	A5	R356	2.425
			A5	R382	2.407
			S3	E361	2.002
			A2	R358	2.590
			S1	D302	2.419
			S1	R358	2.528
			S1	R358	2.072
SQAPA	-6.7	5	A5	Y157	2.267
			S1	T156	2.062
			S1	S106	1.787
			Q2	Y128	2.360
			Q2	D104	2.226
SQSAA	-7.0	1	A4	Y547	2.339

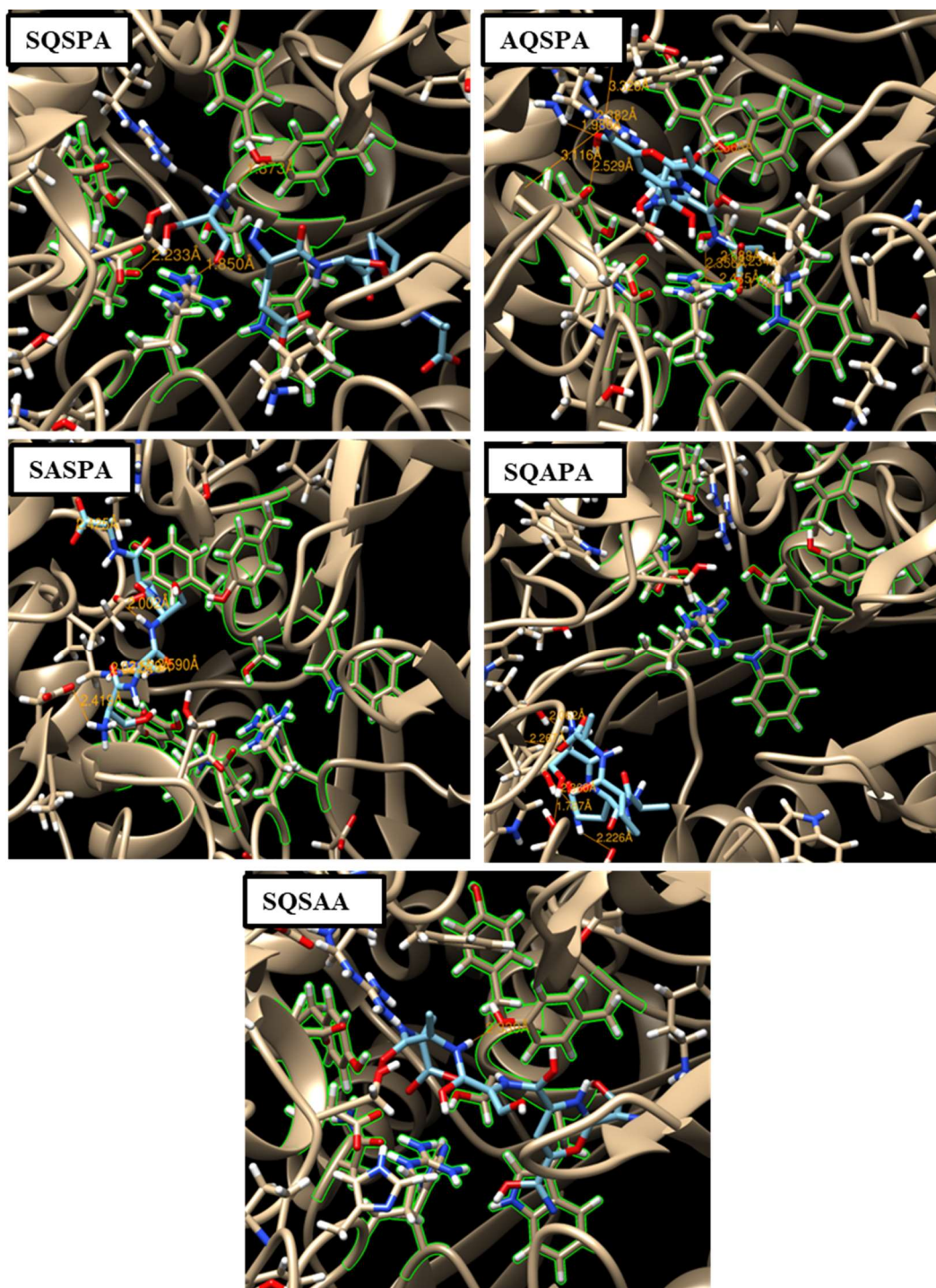


**Fig. 1.** Molecular docking pose of SQSPA and the alanine substituted analogs on human DPP-IV. The orange lines represent the hydrogen bonds with the respective bond distances while the green-highlighted residues indicate the active site. The area for each peptide-DPP-IV interaction was zoomed and presented.

Having established the *in silico* binding potential of the peptides toward DPP-IV, *in vitro* inhibitory studies were then conducted. Compared with diprotin A, the DPP-IV inhibitory of SQSPA was significantly lower ( $p < 0.05$ ) and the alanine substitutions at S1, Q2 and S3 also significantly decreased ( $p < 0.05$ ) the DPP-IV inhibitory activity of the parent

peptide (Table 2). The effect was most pronounced in SQAPA when S3 was substituted. Moreover, the alanine substitution at P4 also decreased the DPP-IV inhibitory activity but the difference was not significant ( $p > 0.05$ ). Overall, the DPP-IV inhibitory activity was in the order of; diprotin A > SQSPA > SQSAA > AQSPA > SASPA > SQAPA (Table 2). In addition to the effects of alanine substitution on the DPP-IV inhibition, it was also important to decipher the role of the alanine substitution on the mechanism of inhibition (Table 2). The SQSPA was a non-competitive inhibitor of the DPP-IV but the alanine substitution at S1, Q2 and S3 shifted the mechanism of inhibition to an uncompetitive inhibition pattern (Table 2). However, SQSAA with alanine substitution at P4 demonstrated a mixed inhibition pattern that was closer to competitive and non-competitive inhibition patterns but not uncompetitive inhibition (Table 2).

**Table 2.** *In vitro* DPP-IV inhibitory activity of SQSPA and its alanine substituted analogs

Peptide/standard	IC <sub>50</sub> for DPP-IV inhibition (mM)	Mechanism of DPP-IV inhibition
SQSPA	3.06 ± 0.30 <sup>b</sup>	Non-competitive
AQSPA	54.67 ± 7.42 <sup>c</sup>	Uncompetitive
SASPA	114.73 ± 1.61 <sup>d</sup>	Uncompetitive
SQAPA	262.40 ± 37.10 <sup>e</sup>	Uncompetitive
SQSAA	3.49 ± 0.23 <sup>b</sup>	Mixed
Diprotin A	0.0035 ± 0.001 <sup>a</sup>	Competitive*

Data are expressed as mean ± SD of two independent experiments done in triplicates. <sup>a-c</sup>Different subscript letters along a column indicates significantly different values (Tukey's-HSD multiple range post hoc test,  $p < 0.05$ ). \* Diprotin A is a known competitive inhibitor of DPP-IV

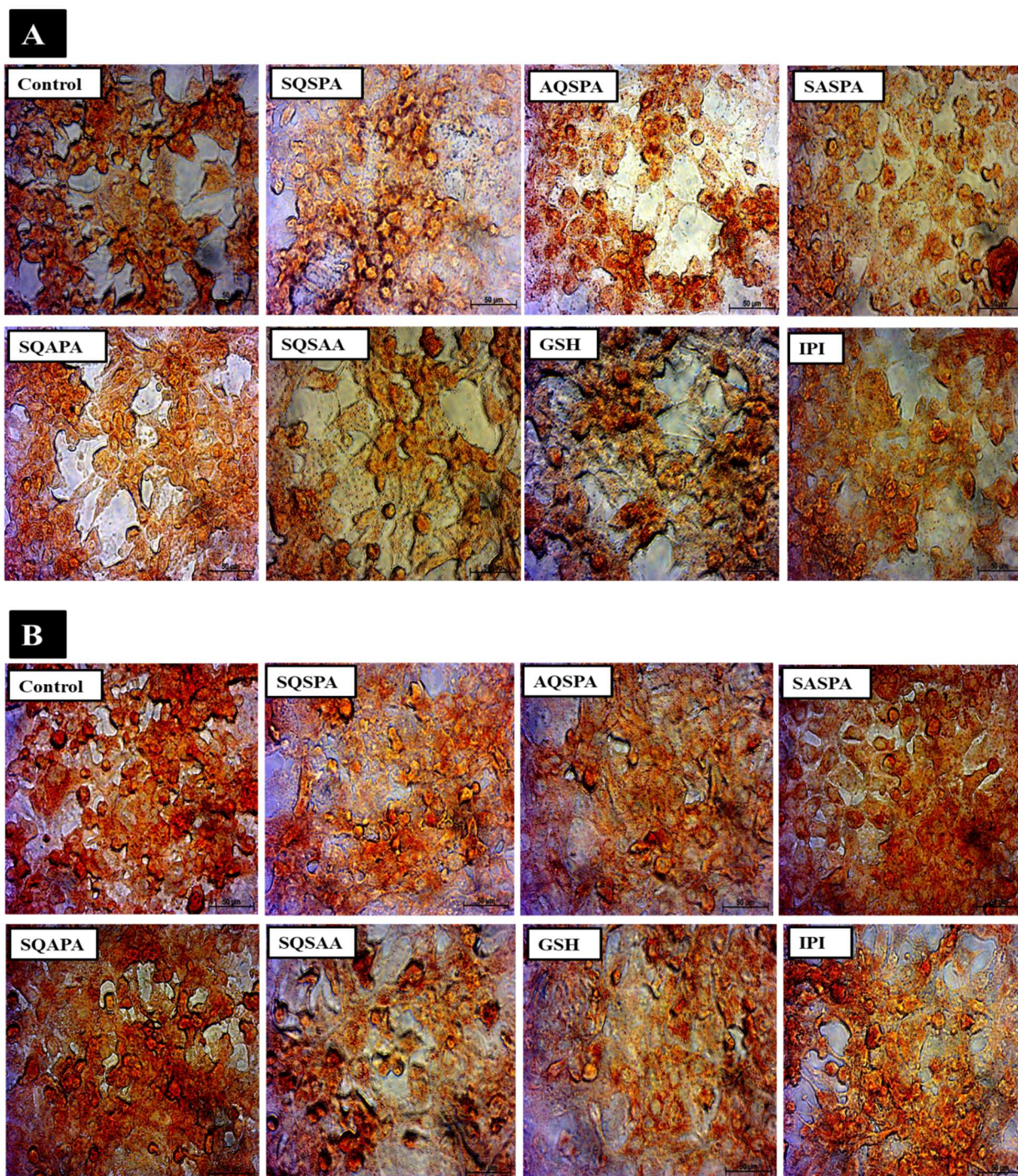


**Fig. 2.** The effects of SQSPA and the alanine substituted analogs (100  $\mu$ M) on lipid accumulation in 3T3-L1 adipocytes during (A) and after (B) the differentiation as evaluated by Oil Red O staining. The cells were photographed at magnification x40.

The ability of 50 and 100  $\mu$ M SQSPA and the analogs to inhibit adipocytes differentiation and lipid accumulation in the 3T3-L1 cell was determined. Representative images of ORO stained adipocytes clearly demonstrated that the 3T3-L1 cells were successfully differentiated to adipocytes (Fig. 2). SQSPA and the analogs did not have

profound effects on adipocyte differentiation and lipid accumulation (Fig. 2A). Quantification of lipid accumulation was supported by qualitative data where the percentage lipid formation in the peptide-treated 3T3-L1 adipocytes were not significantly ( $p < 0.05$ ) different with the control cultures except for exposure to 100  $\mu\text{M}$  of SASPA and SQSAA which contained Q2 and P4 alanine substitutions respectively (Fig. 3A). This identifies the possible relevance of these amino acid positions for the prevention of lipid formation and/or adipocyte differentiation. As the percentage reduction in lipid levels was approximately 8-9% (Fig. 3A), the effect of the peptides on fully differentiated 3T3-L1 adipocytes was further evaluated. Likewise, no marked differences in the number of lipid droplets were observed, with ORO staining (Fig. 2B). However, quantitative analysis showed a significant decrease ( $p < 0.05$ ) in the percentage lipid accumulation in the presence of all the SQSPA analogs (100  $\mu\text{M}$ ) while the parent peptide showed no significant ( $p > 0.05$ ) difference (Fig. 3B). The peptide with Q2 alanine substitution (SASPA) also caused the greatest reduction in lipid levels in differentiated adipocytes (approximately 10% reduction) indicating that the position 2 might be critical to the modulation of cellular lipid content. A slight reduction in lipid levels was also found for the control peptides, GSH and IPI.

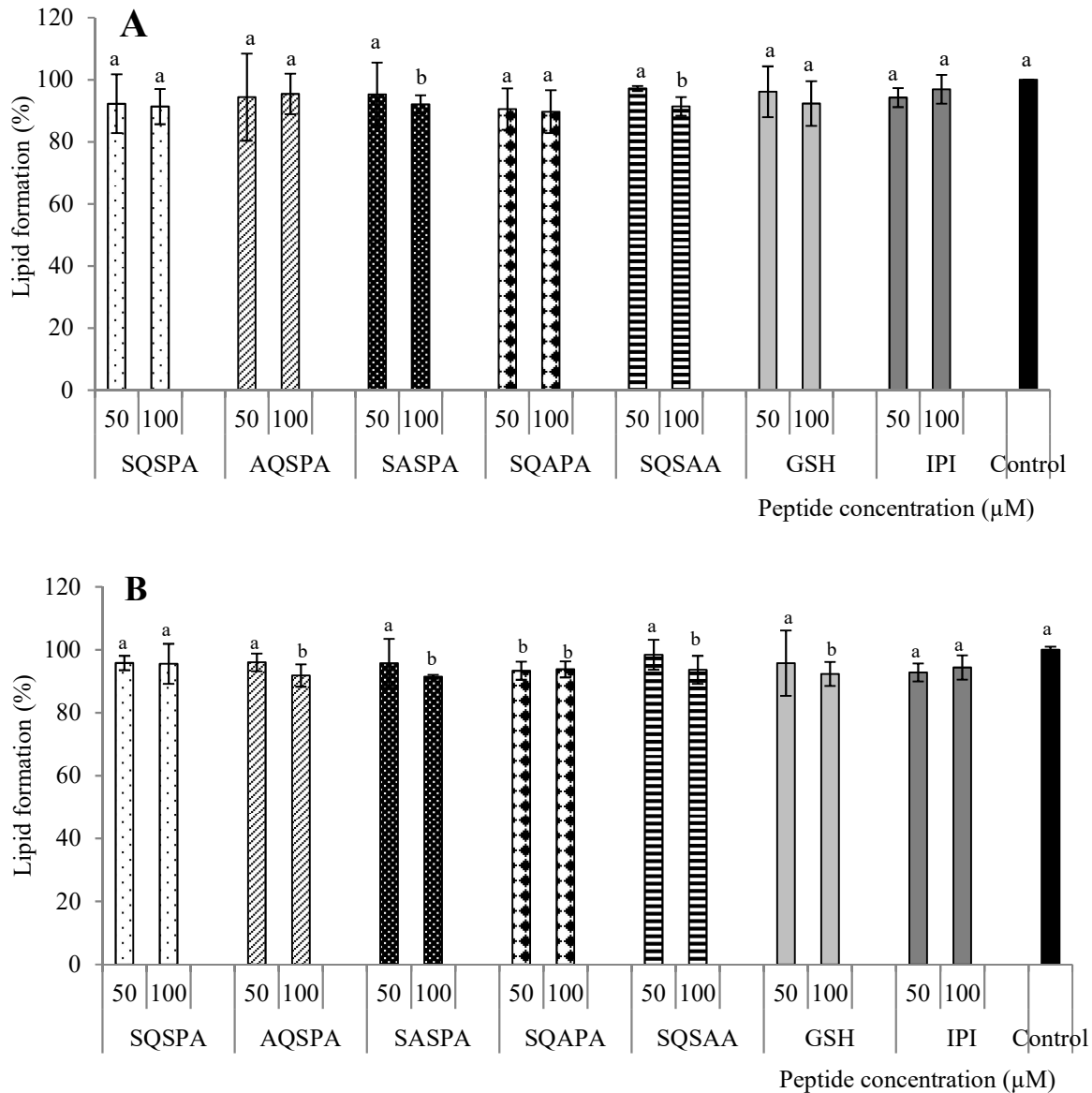


**Fig. 3.** Percentage lipid formation in Oil Red O stained differentiated 3T3-L1 adipocytes during (A) and after (B) the differentiation in the presence of SQSPA and the alanine substituted analogs. The lipid accumulation in the presence of the peptides was expressed as a percentage of the vehicle control. Data are shown as mean  $\pm$  SD of two independent experiments conducted in triplicates. <sup>a-b</sup>Different subscript letters over the bars indicate significantly different values from the control (Tukey's-HSD multiple range post hoc test,  $p < 0.05$ )

Addition of SQSPA and the analogs to differentiated 3T3-L1 adipocytes did not cause significant changes to cell viability (Fig. 4) and the data was similar to GSH and IPI. In contrast, in undifferentiated 3T3-L1 cells, 50  $\mu$ M SQSPA showed significant cytotoxicity ( $p < 0.05$ ). This observation was largely reversed when alanine was substituted at the Q2, S3 and P4 positions. However, for AQSPA with S1 substitution, significant ( $p < 0.05$ )



cytotoxicity with a 30% reduction in viability was observed in undifferentiated cells following exposure to 50 and 100  $\mu\text{M}$  peptide (Fig. 4).

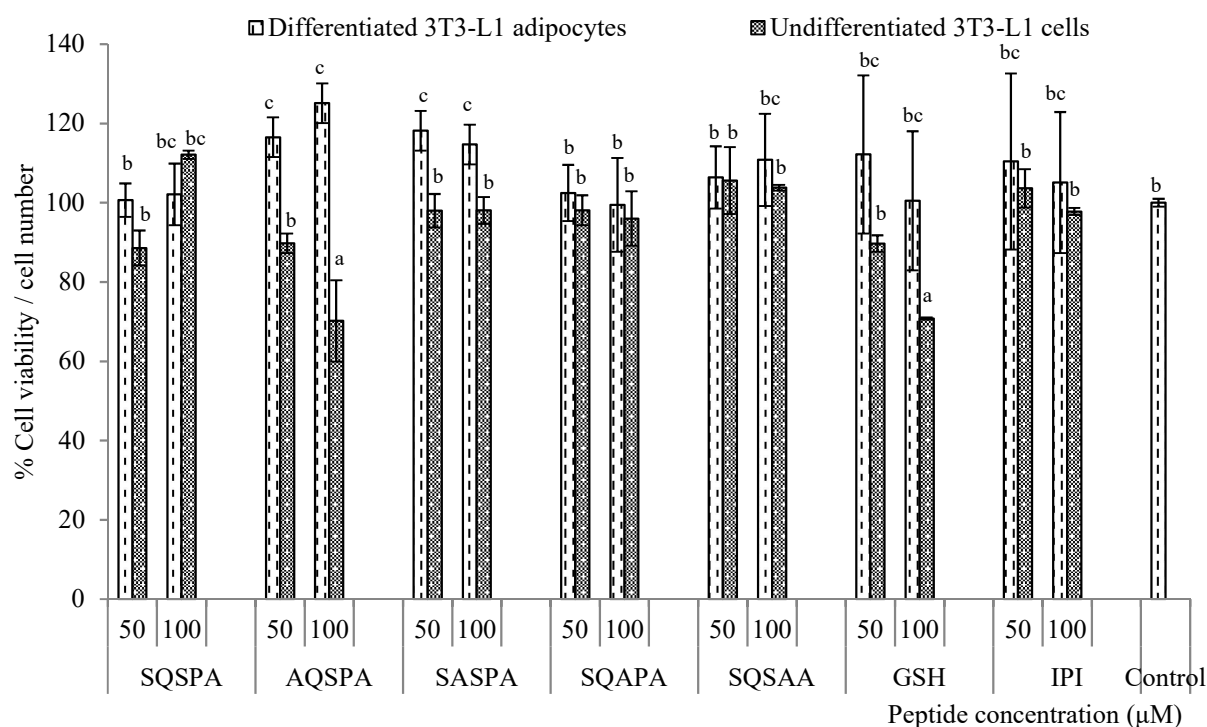


**Fig. 4.** Cytotoxicity profile of SQSPA and the alanine substituted analogs in 3T3-L1 differentiated and undifferentiated cells. Cell viability in the presence of the peptides was expressed as a percentage of the vehicle control. Data are expressed as mean  $\pm$  SD of two independent experiments done in triplicates. <sup>a-c</sup>Different subscript letters over the bars indicate significantly different values (Tukey's-HSD multiple range post hoc test,  $p < 0.05$ )

Similar to IPI, SQSPA and the analogs (except AQSPA) demonstrated a concentration-dependent ability to scavenge MGO with correlations of greater than 0.900 (Fig. 5). Both AQSPA and SASPA had reduced MGO scavenging ability (Fig. 5), denoting the importance of the first 2 amino acid residues. Moreover, the controls (IPI and GSH), SQAPA and SQSAA showed a concentration-dependent linear increase in ROS scavenging ability with correlations greater than 0.800 (Fig. 6). Although no dosage effect was found for SASPA, even at dosage as low as 5  $\mu\text{M}$ , this peptide demonstrated the highest oxygen radical scavenging ability among the peptide analogs, at all the tested concentrations. In fact, with the exception of S1 substitution (AQSPA), the alanine substitutions led to increased oxygen radical scavenging effects of the parent peptide, especially at 30 – 50  $\mu\text{M}$  (Fig. 6).

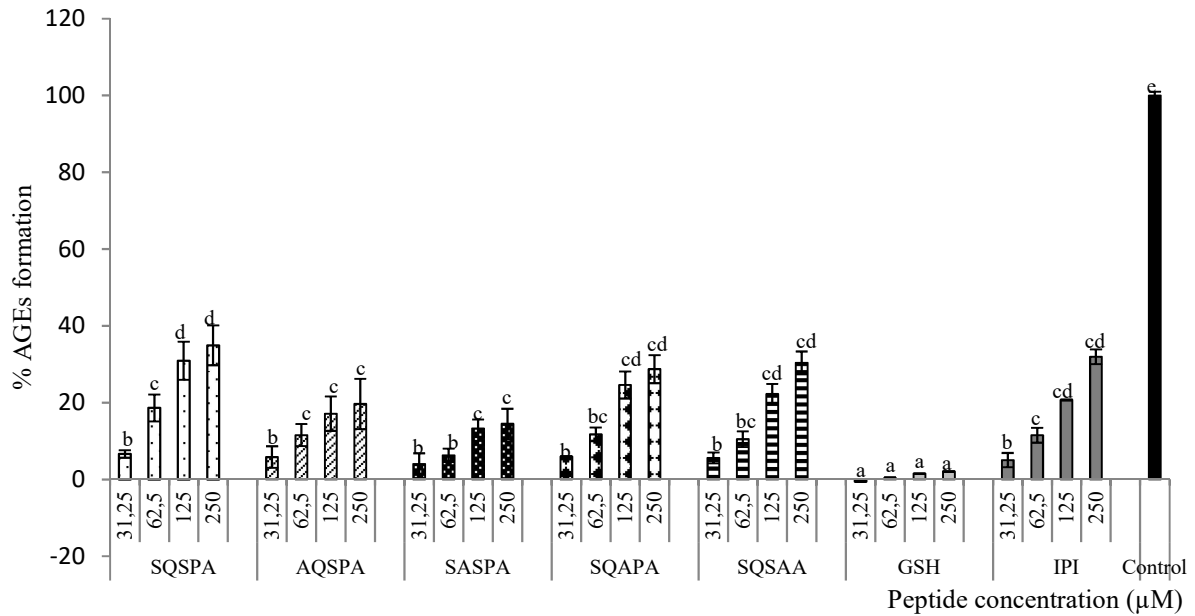


**Fig. 5.** The interaction of various concentrations of SQSPA and the alanine substituted analogs with MGO to generate advanced glycosylated end products. Data are shown as mean  $\pm$  SD of two independent experiments conducted in triplicates. <sup>a-c</sup>Different subscript letters over the bars indicate significantly different values (Tukey's-HSD multiple range post hoc test,  $p < 0.05$ )

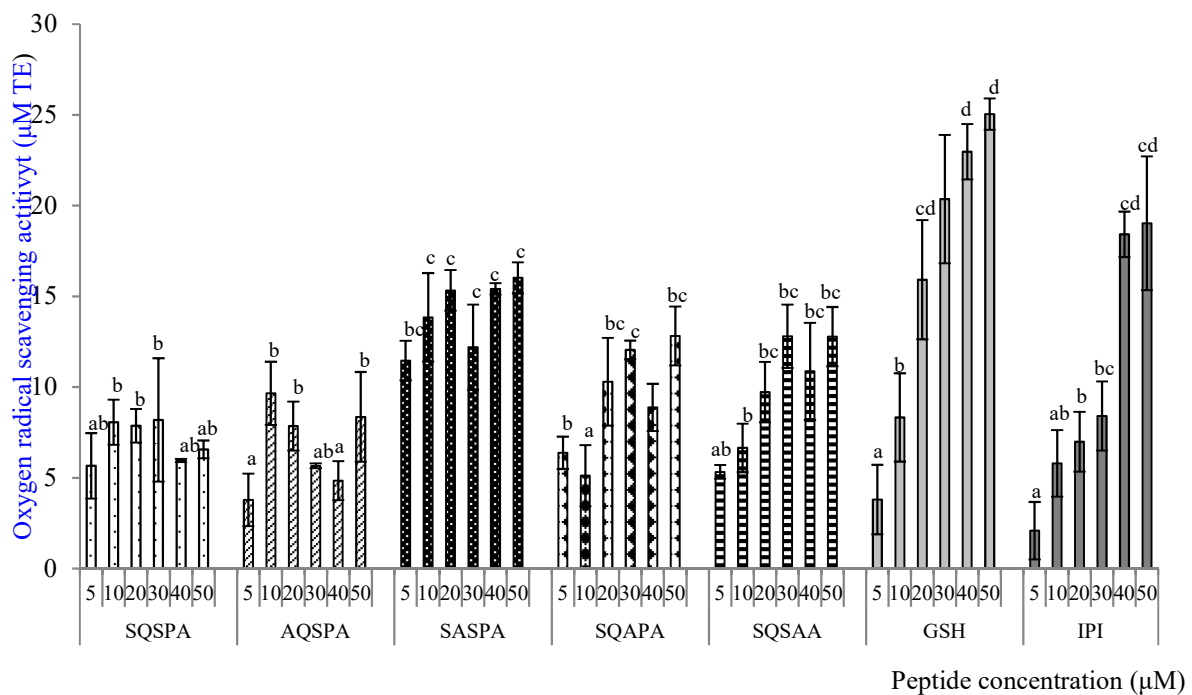


**Fig. 6.** Oxygen radical scavenging effects of various concentrations of SQSPA and the alanine substituted analogs. Data are expressed as mean  $\pm$  SD of two independent experiments done in triplicates. <sup>a-d</sup>Different subscript letters over the bars indicate significantly different values (Tukey's-HSD multiple range post hoc test,  $p < 0.05$ )

SQSPA and the analogs showed a concentration-dependent ability to scavenge NO, with a high degree of correlation ( $> 0.800$ ) for all peptides except AQSPA. Interestingly, alanine substitutions did not lead to significant ( $p > 0.05$ ) change in the activity except at 100  $\mu\text{M}$  where the NO scavenging activity of all the peptide analogs were significantly higher ( $p < 0.05$ ) than the parent peptide, and comparable to the highest concentrations of IPI and GSH (Fig. 7).

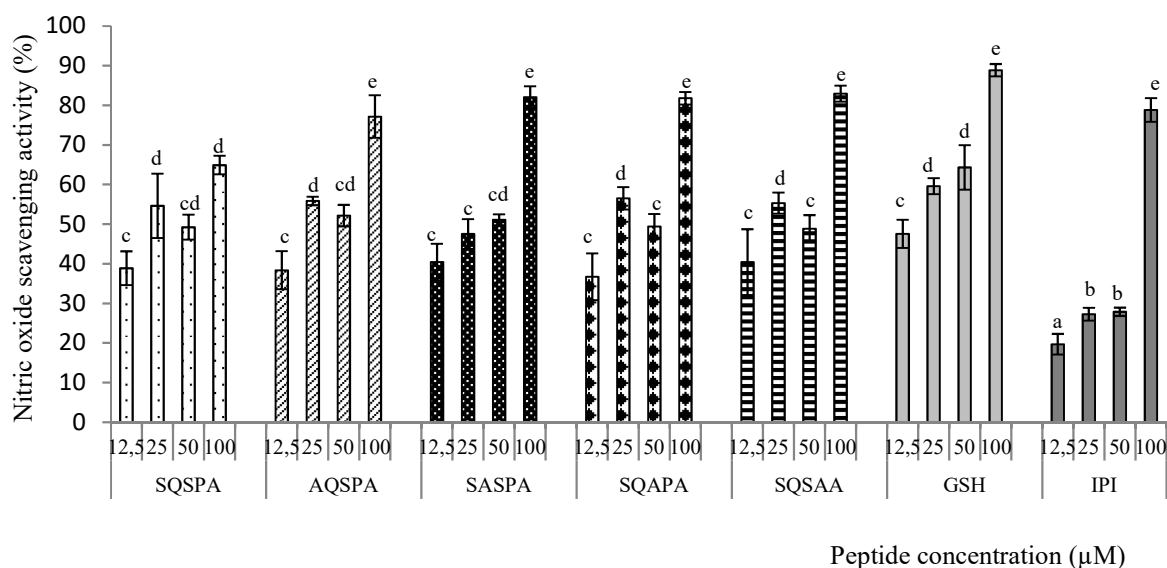


**Fig. 7.** The scavenging potential of various concentrations of SQSPA and the alanine substituted analogs against nitric oxide. The amount of NO scavenged in the presence of the peptides was expressed as a percentage of a control containing all reagents except the peptides. Data are expressed as mean  $\pm$  SD of two independent experiments done in triplicates. <sup>a-e</sup>Different subscript letters over the bars indicate significantly different values (Tukey's-HSD multiple range post hoc test,  $p < 0.05$ )

#### 4. Discussion

Alanine scanning has been a very useful strategy for obtaining unique information on the structure-activity relationship of a peptide and also enables the rational design of peptide analogs with enhanced therapeutic applications and pharmaceutical potential [3, 11, 19]. This is even more useful for disorders such as T2D with multiple therapeutic targets that require multifunctional agents. Herein, we showed that SQSPA, along with the alanine substituted peptide analogs, are multifunctional antidiabetic peptides. Moreover, the S3 residue appears to be a critical position for modulating DPP-IV inhibitory activity of the peptide while the Q2 residue could be the relevant position for inhibiting lipid accumulation in the 3T3-L1 adipocytes as well as MGO and oxygen radical scavenging activities.

In a previous molecular docking study with  $\alpha$ -glucosidase [11], it was observed that the hydroxyl and amide groups of S1 and Q2 respectively, were mainly responsible for preventing effective interactions between the protein and the peptide ligands. Meanwhile, using human DPP-IV as the receptor in the present study, alanine substitutions at S1 and Q2 also increased the binding affinity of the peptide towards the enzyme. This highlights the importance of these residues in mediating the binding of SQSPA to antidiabetic target enzymes. This is further supported by the hydrogen bond interactions where the Q2 happened to be the most hydrogen bonded amino acid. In contrast to previous studies where the presence of proline was an important requirement for DPP-IV inhibitory peptides [23, 24], our observation indicates that the removal of the proline residue (P4) did not affect the binding affinity of the peptide towards DPP-IV. This suggests that the properties of the neighboring amino acid residues, possibly by proximity effect, could be relevant for the proline residue to modulate the flexibility of DPP-IV inhibitory peptides. The human DPP-IV consists of a hydrophobic *S1* pocket made up of Y631, V656, W659, Y662, Y666 and V711 as well as a charged *S2* pocket comprised of R125, E205, E206, F357, S209 and R358 [25]. However, other studies reported three binding pockets: *S1* made up of Y547, S630, Y631, V656, W659, Y662, N710, V711 and H740; *S2* made up of E205, E206, and Y662; and *S3* made up of S209, R358 and F357 [26]. It was interesting to note that SQSPA interacts with residues at both *S1* (Y547 and N710) and *S2* (R125) pockets and evidently, S1 and Q2 alanine substitutions also increased the number of the active site residues involved in the binding event, mainly at the *S2* pocket such as H740, F357, E206 and R358. The foregoing molecular docking data could imply that the hydroxyl and amide side groups of S1 and Q2 respectively, limit the interactions of the parent peptide with sufficient active site residues at the *S2* pocket of the DPP-IV. Consequently, the binding affinity of the peptide towards the enzyme was reduced.

To date, over 2000 bioactive peptides with DPP-IV inhibitory activity have been reported in the literature [24] but none of them was discovered through a similar experimental strategy as used in the present study. Indeed, apart from a study by Nongonierma and FitzGerald [23], structure-activity studies on DPP-IV inhibitory peptides have been rare. It was thus interesting for us to report that hydroxyl side groups of S1 and S3 as well as the amide side group of Q2 are highly essential for the DPP-IV inhibitory activity of the parent peptide because the alanine substitutions at those positions decreased the activity. This is largely contrary to the molecular docking experiments where such alanine substitutions

enhanced the binding affinity. In spite of the unquestionable merits of molecular docking in understanding ligand-receptor interactions, the docking scoring functions do not always correlate with *in vitro* experiments [27]. The DPP-IV is a hydrolase enzyme that requires the presence of water molecules for catalysis, but the water molecules are largely not considered in the molecular docking. Consequently, this might have caused variations in the binding of the peptide ligands to the DPP-IV leading to the observed differences between the molecular docking and *in vitro* results. Nevertheless, with respect to P4, the molecular docking experiment corresponded with the *in vitro* data where it was identified that P4 tends to have no effect on the activity. These observations clearly demonstrated that a combination of *in silico* and *in vitro* studies are essential before a definite conclusion could be made on a structure-activity relationship of a peptide. In spite of these observations, the *in vitro* studies also indicate that the SQSPA and SQSAA are moderately active DPP-IV inhibitory peptides with some capacity to retard the degradation of GLP-1 and GIP which consequently, improves insulin secretory response and glucose homeostasis [12, 28]. With respect to the mechanism of the DPP-IV inhibition, the non-competitive inhibition pattern exhibited by SQSPA suggests that the peptide can bind the free DPP-IV protein or the DPP-IV- Gly-Pro-*p*-nitroanilide (E-S complex) while the uncompetitive inhibition pattern shown by AQSPA, SASPA and SQAPA indicates that these peptides only interact with the E-S complex to inhibit the catalytic process [19]. This clearly demonstrates that the hydroxyl groups of S1 and S3 as well as the amide side group of Q2 are required for the binding of SQSPA to the free DPP-IV protein, highlighting the relevance of these groups to the activity. Overall, these functional groups enhanced the *in vitro* DPP-IV inhibitory activity via increased interaction with the free DPP-IV protein.

Preadipocytes are known to differentiate into mature adipocytes that accumulate excess amounts of triacylglycerols with a concomitant increase in size [29]. Thus, inhibition of both adipogenesis and lipid accumulation are viable strategies for the treatment of T2D [30]. The disadvantage of this strategy is that the inhibitory effect could be reversed once the therapeutic agent is withdrawn. In contrast, increased cytotoxicity with concomitant reduction in the number of adipocytes may have a long term beneficial effect [29]. To some degree, the process of adipocyte differentiation was retarded in the presence of both SASPA and SQSAA, while SASPA was the only peptide that caused significant reduction in the intracytoplasmic lipid accumulation in mature adipocytes. These findings have also identified the role of the amide side chain of Q2 in the modulation of adipogenesis and lipid

accumulation in the 3T3-L1 cells which might be linked to the observed role of the functional group to the DPP-IV inhibitory activity. This is because 3T3-L1 cells express DPP-IV which is released following differentiation and DPP-IV knockdown mimics the growth factor withdrawal that occurs during the early phase of adipocyte differentiation [31]. Moreover, a reduction in DPP-IV is associated with an immature phenotype and an associated reduction in lipid levels. It is thus plausible that the amide side chain of Q2 plays a role in both DPP-IV inhibition, adipogenesis and lipid accumulation in matured adipocytes and these effects are intricately interconnected. Future studies will be important to elucidate the mechanism of action.

Targeting adipocytes and induction of apoptosis have been identified as a potential strategy for reducing T2D associated risks [29] while safety and the lack of toxicity are also important considerations. The cytotoxicity of SQSPA and analogs was determined in both undifferentiated and the differentiated 3T3-L1 cells. Interestingly, all peptides were not cytotoxic to differentiated adipocytes indicating selective targeting and not due to general cytotoxicity. Conversely, SQSPA was cytotoxic to undifferentiated cells but the findings revealed that the amide group of Q2, hydroxyl group of S3 and pyrrolidine side chain of proline were required for toxicity while the hydroxyl group of S1 was largely required for the safety of the parent peptide towards normal mammalian cells.

Considerable experimental and preclinical studies have implicated MGO, generated as a result of excessive hyperglycemia, to be a vital biological player in most aspects of diabetes pathogenesis in addition to being a risk factor for diabetic vascular complications such as dyslipidemia and obesity [15]. Accumulation of MGO generates AGEs which trigger oxidative stress, inflammation and apoptosis. Furthermore, AGEs can reduce NO levels and endothelial NO synthase (eNOS) activity leading to endothelial dysfunction and contributing to microvascular complications [32]. Therefore, besides the observed effects related to DPP-IV, other multifunctional antidiabetic effects can include the scavenging of MGO and ROS and modulating NO levels either directly or indirectly. The MGO selectively modifies the lysine and arginine residues of plasma proteins like albumin, fibrinogen and immunoglobulin [33]. Thus, the presence of smaller peptides with MGO binding capacity such as SQSPA and the analogs (except AQSPA) may have a sparing effect on the plasma proteins. Moreover, the observation that SASPA had the best scavenging potential, further highlights the importance of the Q2 residue. With regards to reduction in ROS and NO levels [34, 35], a linear increase in ROS scavenging was observed with IPI, GSH SQAPA and QSAA while SASPA and

SQSPA scavenged ROS, not in a concentration-dependent manner. In a review, Zou et al. [36] identified that in antioxidant peptides the most common amino acids in the order of abundance were glycine, proline, leucine, alanine, tyrosine and valine while cysteine, methionine, and glutamine were the least abundant. Hydrophobic, aromatic and basic amino acids were identified to contribute significantly to the antioxidant properties of peptides. The presence of proline may account for the antioxidant activity of IPI, while cysteine in GSH acts as a hydrogen donor. The only identified amino acid present in SQSPA and analogs is proline while the antioxidant activity of alanine and glutamine has not been reported. However, the dipeptide alanyl glutamine, in animal and clinical studies has been shown to protect against oxidative stress [38]. Consequently, the observed highest ROS scavenging potential of SASPA suggest that Q2 residue may also play an important role in the oxygen radical scavenging activity of SQSPA although the contribution of SQ and/or QS is unknown.

SQSPA and analogs (except AQSPA), GSH and IPI showed as concentration-dependent ability to scavenge NO, with a high degree of correlation ( $> 0.800$ ). The ability of GSH to scavenge NO with S-nitrothiol formation is well established [38]. Although proline lacks NO scavenging activity [39], cysteine and isoleucine accounts for the scavenging effects of GSH and IPI respectively. Although no literature could be found regarding the NO scavenging activity of serine, alanine and glutamine, SQSPA and analogs presented with NO scavenging activity equivalent to GSH and IPI, indicating either of these amino acids or specific sequences are essential for NO scavenging. However, further investigations with cellular models would provide insights into the physiological relevance of the observed results of ROS and NO scavenging activities of the peptides.

Overall, SQSPA and the alanine substituted analogs could be considered as potential multifunctional antidiabetic peptides because of their abilities to inhibit  $\alpha$ -glucosidase and  $\alpha$ -amylase [11] as well as DPP-IV as observed in this study. Moreover, the structure-activity relationship studies have implicated the amide side chain of Q2, and to a lesser extent, the hydroxyl group of S1 as the most critical positions for modulating the multiple antidiabetic effects of the peptide. Importantly, the study has led to the design of a novel peptide, SASPA, with enhanced multifunctional antidiabetic activity.

## **Acknowledgement**

We acknowledge the National Research Foundation of South Africa (Grant number 91052) and the University of Pretoria for their financial supports. The first author also acknowledges the University of Pretoria for the award of a postdoctoral fellowship position in Biochemistry and Ahmadu Bello University, Zaria, Nigeria for the award of a study fellowship.

## **Conflict of interest**

The authors declare that there are no conflicts of interest

## **Authors' contribution**

MAI and ARMG conceptualised the study while the experiment was designed by MAI, MJB, JCS and ARMG. MAI and JCS conducted the experiments while MAI, MJB, JCS and ARMG performed the data analysis. MAI wrote the manuscript which was edited by MJB, JCS and ARMG

## **References**

- [1] J.L. Lau, M.K. Dunn, *Bioorg. Med. Chem.* 26 (2018) 2700-2707.
- [2] M. Erak, K. Bellmann-Sickert, S. Els-Heindl, A.G. Beck-Sickinger, *Bioorg. Med. Chem.* 26(2018) 2759-2765.
- [3] S. Eustache, J. Leprince, P. Tufféry, *Expert Opin. Drug Disc.* 11 (2016) 771-784
- [4] D.J. Drucker, *Nat. Rev. Drug Disc.* 2019. doi: 10.1038/s41573-019-0053-0.
- [5] M.A. Ibrahim, M.J. Bester, A.W.H. Neitz, A.R.M. Gaspar, *Biomed. Pharm.* 107 (2018) 234 -242.
- [6] A.G. Jamieson, N. Boutard, D. Sabatino, W. D. Lubell, *Chem. Biol. Drug Des.* 81 (2013) 148-165.
- [7] M. Husain, A.L. Birkenfeld, M. Donsmark, K. Dungan, F.G. Eliaschewitz, D.R. Franco, O.K. Jeppesen, I. Lingvay, O. Mosenzon, S.D Pedersen, C.J. Tack, *New Engl. J. Med.* 381 (2019) 841-851.



- [8] N.H. Cho, J.E. Shaw, S. Karuranga, Y. Huang, J.D. da Rocha Fernandes, A.W. Ohlrogge, B. Malanda, *Diabetes Res. Clin. Pract.* 138 (2018) 271-281.
- [9] L. Zhang, Q. Chen, L. Li, J.S.W. Kwong, P. Jia, P. Zhao, W. Wang, X. Zhou, M. Zhang, X. Sun, *Sci. Rep.* 6 (2016) 32649
- [10] M.A. Ibrahim, M.J. Bester, A.W.H. Neitz, A.R.M. Gaspar, *Chem. Biol. Drug Des.* 91 (2018) 370-379.
- [11] M.A. Ibrahim, J.C. Serem, M.J. Bester, A.W.H. Neitz, A.R.M. Gaspar, *Prot. Pept. Lett.* 26 (2019) 403-413.
- [12] E.E. Mulvihill, *Peptides* 100 (2018) 158-164.
- [13] A. Guilherme, J.V. Virbasius, V. Puri, M.P. Czech, *Nat. Rev. Mol. Cell Biol.* 9 (2008) 367–377.
- [14] L. Azul, A. Leandro, P. Boroumand, A. Klip, R. Seiça, C.M. Sena, *Free Rad. Biol. Med.* 146 (2020) 264-274.
- [15] C.G. Schalkwijk, C.D.A. Stehouwer, *Physiol. Rev.* 100 (2020) 407 - 607
- [16] T. S. Assmann, L.A. Brondani, A.P. Bouças, J. Rheinheimer, B.M. de Souza, L.H. Canani, A.C. Bauer, D. Crispim, *Nitric Oxide*, 61 (2016) 1-9.
- [17] E.F. Pettersen, T.D. Goddard, C.C. Huang, G.S. Couch, D.M.Greenblatt, E.C. Meng, T.E. Ferrin, *J. Comput. Chem.* 25 (2004) 1605 – 1612.
- [18] O. Trott, A.J. Olson, *J. Comput. Chem.* 31 (2010) 455–461.
- [19] M.A. Ibrahim, J.C. Serem, M.J. Bester, A.W.H. Neitz, A.R.M. Gaspar, *Int. J. Biol. Macromol.* 122 (2019b) 104-114.
- [20] M.A. Siddiqui, S. Rasheed, Q. Saquib, A.A. Al-Khedhairy, M.S. Al-Said, J. Musarrat, M.I. Choudhary, *BMC Complement. Altern. Med.* 16 (2016) 276.
- [21] B. Ou, D. Huang, M. Hampsch-Woodill, J.A. Flanagan, E.K. Deemer, *J. Agric. Food Chem.* 50 (2002) 3122–3128.

- [22] D. Giustarini, R. Rossi, A. Milzani, I. Dalle-Donne, *Methods Enzymol.* 440 (2008) 361–380.
- [23] A.B. Nongonierma, R.J. FitzGerald, *Peptides* 79 (2016) 1-7.
- [24] R. Liu, J. Cheng, H. Wu, *Int. J. Mol. Sci.* 20 (2019) 463.
- [25] L. Juillerat-Jeanneret, *J. Med. Chem.* 57 (2014) 2197–2212.
- [26] B.R. Kim, H.Y. Kim, I. Choi, J.B. Kim, C.H. Jin, A.R. Han, *Molecules* 23 (2018) 1998.
- [27] D. Ramirez, J. Caballero, *Int. J. Mol. Sci.* 17 (2016) 525
- [28] C.F. Deacon, *Front. Endocrinol.* 10 (2019) 80.
- [29] S.R. Balusamy, K. Veerapan, A. Rajan, Y. Kim, D.K. Chellapan, K. Dua, J. Lee, H. Perumalsamy, *Phytomedicine.* 66 (2020) 153129.
- [30] S.Y. Sim, Y.E. Shin, H.K. Kim, *Nutr. Res.*, 65 (2019) 54-62.
- [31] P. Zilleßen, J. Celner, A. Kretschmann, A. Pfeifer, K. Racke P. Mayer, *Sci. Rep.* 6 (2016) 23074.
- [32] K. Maejima, S. Nakano, M. Himeno, S.I. Tsuda, H. Makiishi, T. Ito, A. Nakagawa, T. Kigoshi, T. Ishibashi, M. Nishio, K. Uchida, *J. Diabetes Complications* 15 (2001) 135-143.
- [33] R.S. Tupe, N. Bangar, A. Diwan, D. Changale, S. Chooudhary, S. Chaware, *Mol. Biol. Rep.* 47 (2020) 521-531.
- [34] A. Megenta, S. Greco, M.C. Capogrossi, C. Gaetano, F. Martelli, *Biomed. Res. Int.* 2014 (2014) 193095. doi: 10.1155/2014/193095
- [35] M. Gliozzi, M. Scicchitano, F. Bosco, V. Musolino, C. Caressi, F. Scarano, J. Maiuolo, S. Nucera, A. Maretta, S. Paone, R. Mollace, S. Ruga, M.C. Zito, R. Macri, F. Oppedisano, E. Palma, D. Salvemini, C. Muscoli, V. Mollace, *Int. J. Mol. Sci.* 20 (2019) 3294

- [36] T.B. Zou, T.P. He, H.B. Li, H.W. Tang, E.Q. Xia, *Molecules* 21 (2016) 72
- [37] B. Matilla, J. Ortíz, J. González-Gallego, M.J. Tuñón, *Nutrition* 16 (2000) 125-128.
- [38] A. Schrammel, A.C.F. Gorren, K. Schmidt, S. Pfeiffer, B. Mayer, *Free Rad. Biol. Med.* 34 (2003) 1078-1088.
- [39] S. Signorelli, C. Imparatta, M. Rodriguez-Ruiz, O. Borsani, F.J. Corpas, J. Monza, *Funct. Plant Biol.* 43 (2016) 870-879.